BBA - Molecular Cell Research 1867 (2020) 118723

Contents lists available at ScienceDirect

BBA - Molecular Cell Research

journal homepage: www.elsevier.com/locate/bbamcr

Cathepsin C is a novel mediator of podocyte and renal injury induced by hyperglycemia

Irena Audzeyenka[a,b,*], Patrycja Rachubik[a], Dorota Rogacka[a,b], Marlena Typiak[a], Tomasz Kulesza[a], Stefan Angielski[a], Michał Rychłowski[c], Magdalena Wysocka[b], Natalia Gruba[b], Adam Lesner[b], Moin A. Saleem[d], Agnieszka Piwkowska[a,b]

[a] Laboratory of Molecular and Cellular Nephrology, Mossakowski Medical Research Centre, Polish Academy of Sciences, Gdansk, Poland
[b] Faculty of Chemistry, University of Gdansk, Poland
[c] Intercollegiate Faculty of Biotechnology, University of Gdansk - Medical University of Gdansk, Poland
[d] Bristol Renal, University of Bristol, United Kingdom

ARTICLE INFO

Keywords:
Albumin permeability
Cathepsin C
Diabetic nephropathy
Hyperglycemia
Podocytes

ABSTRACT

A growing body of evidence suggests a role of proteolytic enzymes in the development of diabetic nephropathy. Cathepsin C (CatC) is a well-known regulator of inflammatory responses, but its involvement in podocyte and renal injury remains obscure. We used Zucker rats, a genetic model of metabolic syndrome and insulin resistance, to determine the presence, quantity, and activity of CatC in the urine. In addition to the animal study, we used two cellular models, immortalized human podocytes and primary rat podocytes, to determine mRNA and protein expression levels via RT-PCR, Western blot, and confocal microscopy, and to evaluate CatC activity. The role of CatC was analyzed in CatC-depleted podocytes using siRNA and glycolytic flux parameters were obtained from extracellular acidification rate (ECAR) measurements. In functional analyses, podocyte and glomerular permeability to albumin was determined. We found that podocytes express and secrete CatC, and a hyperglycemic environment increases CatC levels and activity. Both high glucose and non-specific activator of CatC phorbol 12-myristate 13-acetate (PMA) diminished nephrin, cofilin, and GLUT4 levels and induced cytoskeletal rearrangements, increasing albumin permeability in podocytes. These negative effects were completely reversed in CatC-depleted podocytes. Moreover, PMA, but not high glucose, increased glycolytic flux in podocytes. Finally, we demonstrated that CatC expression and activity are increased in the urine of diabetic Zucker rats. We propose a novel mechanism of podocyte injury in diabetes, providing deeper insight into the role of CatC in podocyte biology.

1. Introduction

Increased activity of proteolytic enzymes has been suggested to promote injury to the renal filtration barrier and renal function [1]. The mechanisms underlying protease-mediated damage comprise the deregulated proteolysis of glomerular basement membrane (GBM) components, proteolysis of non-GBM proteins, and alteration of glomerular metabolism [1]. Immune cells are thought to be the main source of active proteases, but recent findings have highlighted the role of renal cells in the production of a wide range of proteases in response to different stimuli. Proteases play an important role in the physiology and function of podocytes, and some of them (cathepsin L, D, calpain, caspase 1, metalloproteases 2 and 9, dipeptidyl peptidase 4 [DPP-4]) are well-described in the literature [2–6].

For example, activation of cathepsin L-mediated proteolysis has been suggested as one of the major causes of foot process effacement and proteinuria [7]. Moreover, DPP-4 has been shown to be expressed in podocytes in patients with diabetic nephropathy, but not in healthy individuals [8]. In addition to a range of proteolytic enzymes, podocytes also express protease-activated receptors (PARs) 1–4, and the

Abbreviations: BSA, Bovine Serum Albumin; CatC, Cathepsin C; DMEM, Dulbecco's Modified Eagle Medium; ECAR, Extracellular Acidification Rate; FBS, Fetal Bovine Serum; GBM, Glomerular Basement Membrane; GLUT4, Facilitated Glucose Transporter member 4; HG, high glucose concentration medium (30 mM); PFA, paraformaldehyde; PMA, Phorbol 12-Myristate 13-Acetate; SFM, Serum-Free Medium; SG, standard glucose concentration medium (10 mM)

* Corresponding author at: Laboratory of Molecular and Cellular Nephrology, Mossakowski Medical Research Centre, Polish Academy of Sciences, Wita Stwosza St. 63, 80-308 Gdansk, Poland.
E-mail address: iaudzeyenka@imdik.pan.pl (I. Audzeyenka).

https://doi.org/10.1016/j.bbamcr.2020.118723
Received 14 January 2020; Received in revised form 8 April 2020; Accepted 9 April 2020
Available online 14 April 2020

roles of PAR1, PAR2, and PAR3 have been studied in podocytes thus far [9–11]. However, to the best of our knowledge, no research on cathepsin C (CatC) in podocytes has been published.

CatC (EC 3.4.14.1), also known as dipeptidyl peptidase 1, is a tetrameric cysteine protease with a molecular weight of ~200 kDa [12,13]. It is expressed ubiquitously, with the most prominent expression in the lungs, placenta, spleen, and kidneys [14]. CatC is synthesized as a proteolytically inactive zymogen (~52 kDa), and then processed in a series of proteolytic cleavages to produce a mature form of the enzyme, which is composed of three subunits: N-terminal exclusion domain chain with three glycosylation sites (~16 kDa), a catalytic heavy chain with one glycosylation site (~23 kDa), and a light chain (~7.5 kDa) [12,13]. The functional tetramer is made of four identical heterotrimers. At a slightly acidic pH (4.5–6.8), CatC exhibits broad substrate activity, and its catalytic action involves the removal of dipeptides from the N-terminus of the substrate [15]. The most characterized CatC substrates belong to the granule-associated serine proteases: cathepsin G, proteinase 3, human neutrophil elastase, mast cell chymase, and granzymes A and B [16]. The upstream CatC activators include cathepsins L, S, V, and K, which are proposed to play a role in its proteolytic maturation [17,18].

Alterations in the concentration and activity of different proteases in urine have been reported in diabetic patients and experimental animal models, some of which are proposed to serve as biomarkers of renal complications in diabetes, including cathepsin B and D, kallikrein 4, and DPP-4 [19–21]. Moreover, non-obese diabetic (NOD) mice have been reported to be partially protected from the development of diabetes when lacking cathepsin S (*Ctss*$^{-/-}$) or cathepsin B (*Ctsb*$^{-/-}$), whereas cathepsin L knockouts (*Ctsl*$^{-/-}$) are fully resistant to diabetes [22]. Elevated expression and urinary activity of DPP-4 has been linked to renal fibrosis in diabetic nephropathy, and DPP-4 inhibitors are used as potent hypoglycemic drugs [5,23,24]. Urinary activity of metalloproteinases 2 and 9 has been also associated with renal impairment in diabetes [25].

Structural and functional impairment of podocytes, which constitute the outer layer of the renal glomerular filtration barrier, play a pivotal role in the development of diabetic nephropathy [26]. Podocytes are non-dividing and uniquely insulin-sensitive cells in the glomerulus of the kidney, in which insulin signaling is not only oriented to the stimulation of glucose uptake, but also promotes cytoskeletal rearrangements, regulating albumin permeability [27]. In the present study, we demonstrate the presence of CatC in podocytes and shed light on its role in podocyte function in a hyperglycemic environment. Using Zucker rats (Crl: ZUC-Lepr$^{fa/fa}$), which are a popular model of insulin resistance and metabolic syndrome, we also show that the quantity and activity of CatC in urine can serve as a marker of renal damage.

2. Materials and methods

2.1. Human podocyte cell line

Conditionally immortalized human podocytes (kind gift from Moin A Saleem) were cultured as described previously [28]. The cells were cultured at 33 °C to proliferate, and then transferred to 37 °C to differentiate for 10–16 days. The expression of podocyte markers (nephrin, podocin, podocalyxin) was checked, and mycoplasma tests (MycoSensor PCR Assay Kit, Agilent) were performed regularly to ensure cell line purity.

2.2. Primary rat podocyte culture

Female Wistar rats weighing ~120 g were used to isolate glomeruli and set up the primary podocyte culture. All of the steps and protocol were described previously [29]. Cell phenotype was verified by immunofluorescence using nephrin and synaptopodin antibodies. All experiments involving animals were approved by the Local Bioethics Committee (no. 10/2015) and performed in accordance with directive 2010/63/EU.

2.3. Experimental animals and metabolic studies

Obese (n = 6) and lean (n = 6) male Zucker rats were obtained from Charles River, Jackson Laboratory (USA). Animals were maintained on a 12-h light and dark cycle with free access to standard pellet diet and tap water. Experiments were performed on 12-week-old rats kept in separate metabolic cages for 48 h with free access to a regular pellet diet and drinking water. The rats were allowed to acclimatize during the first 24 h, and then during the next 24 h urine was collected and urinary albumin, creatinine, nephrin, and cystatin C excretion measured using the Rat ALB (Albumin) ELISA Kit (*E*-EL-R0362, Elabscience), Creatinine Urinary Detection Kit (EIACUN, Invitrogen), Rat NPHN (Nephrin) ELISA Kit (ER1196, FineTest), and Rat Cys-C (Cystatin C) ELISA kit (ER0891, FineTest). Fasting glucose was measured in whole blood samples using a glucose oxidase method (Accu-Chek Performa, Roche Diagnostics GmbH). All procedures were approved by Local Bioethics Committee (no. 10/2015) and applied in accordance with directive 2010/63/EU.

2.4. Isolation of rat glomeruli for physiological studies

Zucker rat kidneys were removed and placed in ice-cold PBS (pH 7.4) supplemented with 0.49 mM $MgCl_2$, 0.9 mM $CaCl_2$, and 5.6 mM glucose. The renal capsule was removed and the cortex minced with a razor blade, and then pressed through a system of sieves with decreasing pore diameters (250, 125, and 75 μm). The whole procedure was performed on ice and was completed in < 1 h.

2.5. Glomerular permeability to albumin in vitro

The volume response of glomerular capillaries to an oncotic gradient generated by defined concentrations of albumin was analyzed as described previously [30]. Briefly, the glomeruli were affixed to 0.1% poly-L-lysine-coated plates and incubated in PBS containing 5% bovine serum albumin (BSA) with 0.49 mM $MgCl_2$, 0.9 mM $CaCl_2$, and 5.6 mM glucose for 15 min at 37 °C. The buffer was replaced with fresh buffer containing 1% BSA to produce an oncotic gradient across the glomerular capillary wall (5% BSA in the lumen vs. 1% BSA in the bathing medium). Control glomeruli were treated with equivalent volumes of medium containing 5% BSA (no oncotic gradient). The glomerular volume changes were recorded by videomicroscopy (Olympus IX51) before and after an oncopressive medium change. Glomerular volume (V) was calculated from the surface area (A) of the glomerulus using the following formula using CellSens Dimension software (Olympus): $V = [4/3A\sqrt{A/\pi}]/10^6$. Volume changes (ΔV) were calculated as $\Delta V = (V_{final} - V_{initial})/V_{initial}$ based on the direct relationship between the increase in ΔV and oncotic gradient applied across the capillary wall. This principle was used to calculate the reflection coefficient of albumin (σ_{alb}), defined as the ratio of the ΔV for the experimental glomeruli to the ΔV of control glomeruli in response to identical oncotic gradients, where $\sigma_{alb} = \Delta V_{experimental}/\Delta V_{control}$. The reflection coefficient of albumin (convectional P_{alb}) was used to calculate the glomerular capillary permeability to albumin ($1 - \sigma_{alb}$), which describes the movement of albumin consequent to water flow. At least three glomeruli from obese (n = 6) and lean (n = 6) Zucker rats were studied in each experiment.

2.6. Real-time PCR

Total cellular RNA from cultured podocytes was isolated using the RNeasy Mini Kit (Qiagen) including an on-column DNAse treatment step (RNase-Free DNase Set, Qiagen). The quantity and purity of RNA were determined by NanoDrop® (Thermo Scientific). After the reverse

Table 1
Primers and probes used in real-time PCR experiments.

Gene	Accession no.	Primer sequences (5′-3′)	Probe sequences (5′-3′)	Product
Cathepsin C (human)	NM_001814.6	F: acctgccaactgcacctatc R: taagtggtcaccttgctgcc	acctgctg	273 bp
Actin beta (human)	X00351.1	F: attggcaatgagcggttc R: ggatgccacaggactcca	cttccagc	76 bp
Cathepsin C (rat)	NM_017097.1	F: ctgccaactgcacttaccc R: actacctttttcttctgttggttcc	acctgctg	115 bp
Actin beta (rat)	NM_031144.3	F: aggcccctctgaacccta R: ggggtgttgaaggtctcaaa	cgtgaaaagatg	70 bp

Table 2
Primary antibodies used in experiments.

Antibody	Clonality	Dilution	Source
Cathepsin C	monoclonal	1:400	Santa Cruz sc-74,590
Nephrin	polyclonal	1:1000	Sigma Aldrich PRS2265
Actin	monoclonal	1:10000	Sigma Aldrich A3853
GLUT4	polyclonal	1:500	Sigma Aldrich SAB4300667
Cofilin	polyclonal	1:400	Sigma Aldrich SAB4500148
p-Cofilin (pSer^3)	polyclonal	1:3000	Sigma Aldrich SAB4504370

Table 3
Statistical tests used in the experiments.

Experiment	Statistical analyses
ΔΔCt (real-time PCR)	unpaired *t*-test; Mann Whitney test
FITC-albumin permeability (podocytes)	
Glomerular permeability to albumin	unpaired *t*-test
ELISA	Mann Whitney test
CatC activity assays	paired *t*-test, one-way ANOVA
Densitometry	Mann Whitney test, paired *t*-test,
ECAR	unpaired *t*-test

transcription of isolated RNA, the levels of specified mRNA transcripts were analyzed by real-time PCR performed in a LightCycler 480 (Roche) using gene-specific intron-spanning primers and fluorescent hydrolysis probes. The results were quantified by the ΔΔCt method with β-actin as an internal control. The amplified products were separated in a 2.5% agarose gel and imaged by the GelDoc-It Imaging System (UVP, Cambridge, UK). Primers and probes are characterized in Table 1.

2.7. Western blotting

Podocyte cell lysates were prepared as described previously [29]. Equal amounts of total protein (25 μg per well) were subjected to SDS-PAGE and then immunoblotted on PDVF membranes. Urinary samples were centrifuged (20 min, 18,000 ×*g*, 4 °C), mixed with SDS running buffer, heated 5 min at 95 °C, and run on a 10% gel at volumes normalized to 24 h urine volumes for each tested rat. Densitometric quantification of the bands was performed with ImageJ software. The primary antibodies used are described in Table 2.

2.8. Immunofluorescent staining

Podocytes were cultured on glass coverslips coated with type I collagen. Differentiated cells were fixed in 4% paraformaldehyde, permeabilized in 0.1% Triton-X 100, and blocked with 3% BSA in PBS. Next, podocytes were incubated for 2 h with primary antibodies diluted in 3% BSA. Blocking solution was used instead of primary antibodies as non-specific staining controls. After extensive washing with PBS and incubation with secondary fluorescent antibodies, the coverslips were mounted to slides using Fluoromount Aqueous Mounting Medium (Sigma-Aldrich). The specimens were imaged using a confocal laser scanning microscope (Leica SP8X).

2.9. Determination of cathepsin C activity

2.9.1. Sample preparation

Immortalized human podocytes were cultured on 10-cm Petri dishes at 33 °C to ~80% confluency and then differentiated at 37 °C for 12–14 days. Primary rat podocytes were grown in collagen I-coated T75 flasks at 37 °C for 12–14 days (1.2×10^6 cells/flask). A day before the experiment, cell culture medium was replaced with 4 ml EX-Cell Serum Free Medium (Sigma) in both cell types. The next day, supernatants were collected and cells lysed in 300 μl of lysis buffer (20 mM Tris, 140 mM NaCl, 2 mM EDTA, 10% glycerol, 0.001% NP-40, 2 mM DTT, pH 8.0). Protein concentration was assessed in all samples. Twenty-four hour urine samples were collected from Zucker rats in metabolic cages as described above.

2.9.2. Measurement of cathepsin C activity

To measure the active form of human CatC, a fluorescent substrate was used [16]. In the activity assay, the substrate Thi-Ala(Mca)-Ser-Gly-Tyr(3-NO_2)-NH_2 (7.5 μM) was incubated at 37 °C with sample diluted in 25 mM MES, 50 mM NaCl, 2 mM DTT (pH 6). As a specific activity control, the sample was pre-incubated for 15 min with 5 μM of Thi-Phe-CN, a selective CatC inhibitor [31], at 37 °C in the buffer mentioned above. The following sample amounts were used: 1.5 μl of cell lysate, 80 μl of cell supernatant, 80 μl of urine. The change in fluorescence intensity was observed for 90 min (λ_{ext} = 320 nm and λ_{em} = 450 nm). All measurements were performed in triplicate and recorded on a CLARIOStar (BMG Labtech Germany).

2.10. Albumin permeability of the podocyte monolayer

Transepithelial albumin permeability was evaluated by measuring FITC-labeled BSA diffusion across a podocyte monolayer as described previously [32], with minor modifications [29]. Podocytes were seeded on type IV collagen-coated cell culture inserts (BD Biosciences) placed in 24-well plates. Podocytes were transfected with control and target siRNAs and incubated under control or experimental conditions. On the day of the experiment, the medium was replaced with serum-free medium (SFM) for 2 h. The medium in the upper compartment was then replaced with 0.3 ml of fresh SFM, and the medium in the lower compartment with 1.5 ml of SFM containing 1 mg/ml FITC-albumin. After 1 h incubation, 200 μl of solution from the upper chamber was transferred to a 96-well plate and the FITC-albumin concentration determined based on the absorbance at 490 nm in a plate spectrophotometer (ELx808, BioTek, USA).

2.11. siRNA transfection

One day before transfection, the podocyte culture medium was replaced with antibiotic-free RPMI 1640 supplemented with 10% FBS. On the day of the experiment, podocytes were incubated for 7 h with CatC siRNA (80 nM) or scrambled siRNA (80 nM) reconstituted in Opti-MEM

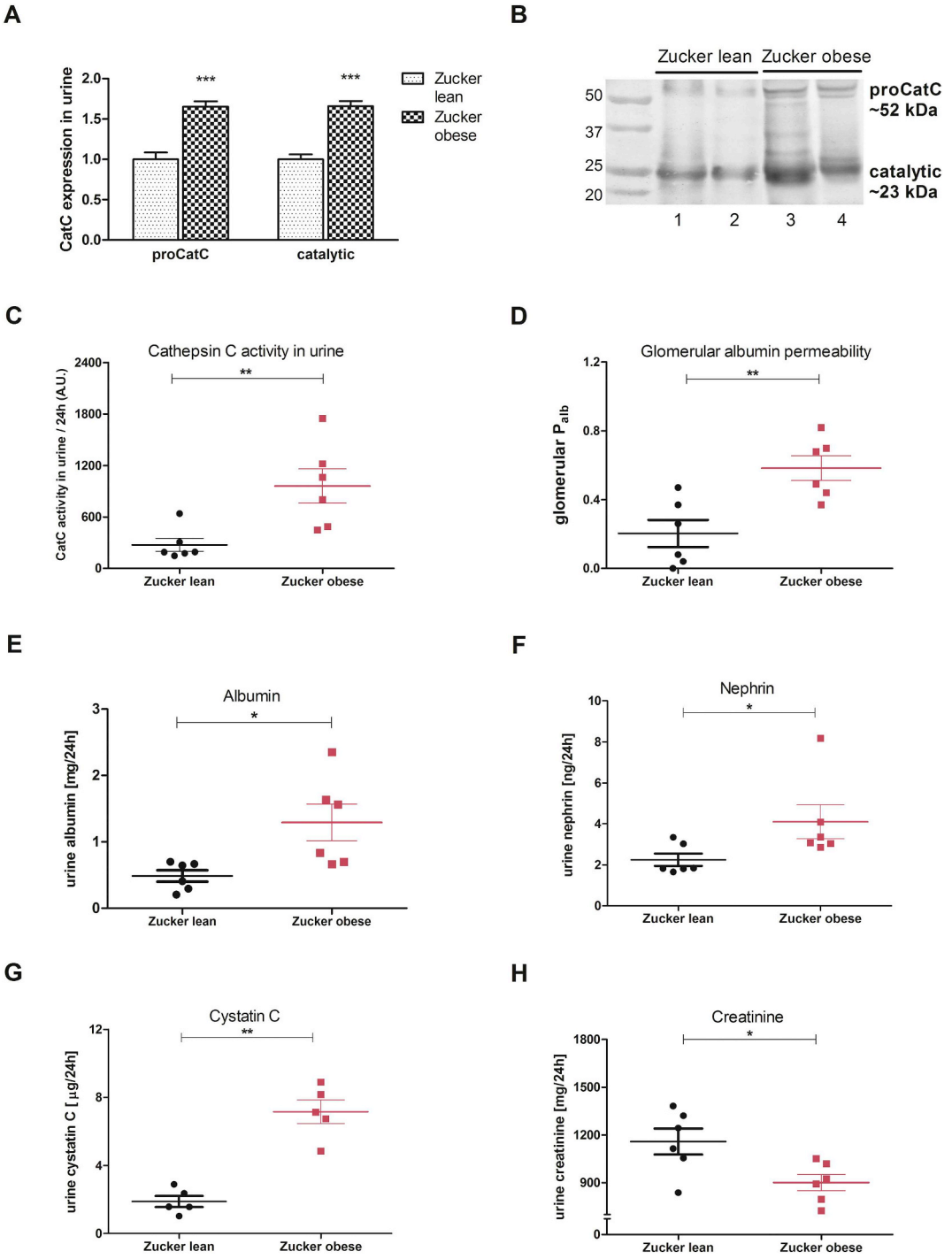

Fig. 1. Cathepsin C expression and activity is elevated in urine from obese Zucker rats. (A) Expression of both pro-cathepsin C and its catalytic form was increased in urine from obese rats (***$p < .001$ vs. lean, Mann-Whitney test, $n = 11–16$). (B) Representative blot showing the increased quantity of CatC in urine from obese rats (numbers 1–4 indicate different animals involved in the experiment). The volume of urine samples run in a gel was adjusted to constitute 0.07% of the volume of 24-h urine collection. (C) Cathepsin C activity was significantly upregulated in obese rats (**$p < .01$, $n = 6$, Mann-Whitney test). (D) Increased permeability to albumin was observed in glomeruli isolated from obese rats (**$p < .01$, n = 6, Mann-Whitney test). (E) Urine albumin was elevated in obese rats (*$p < .05$, n = 6, Mann-Whitney test). (F) Obese rats had higher urine nephrin levels (*$p < .05$, n = 6, Mann-Whitney test). (G) Cystatin C is markedly augmented in the urine of obese rats (**$p < .01$, $n = 5$, Mann-Whitney test). (H) Creatinine levels in the urine of obese Zucker rats were lower than in their lean counterparts (*$p < .05$, n = 6, Mann-Whitney test). A.U., arbitrary units.

(Gibco) containing Transfection Reagent (Santa Cruz Biotechnology). Equal volumes of RPMI 1640 supplemented with 2-fold higher FBS and antibiotic concentrations were added for the next 24 h. Gene silencing was monitored at the protein level by Western blotting.

2.12. Measurement of the extracellular acidification rate (ECAR)

Podocytes were cultured on 8-well culture microplates (Agilent) coated with Rat Tail Collagen-I Solution (Sigma). On the day of the experiment, the growth medium was replaced with assay medium (minimal DMEM supplemented with 2 mM L-glutamine) and the cells

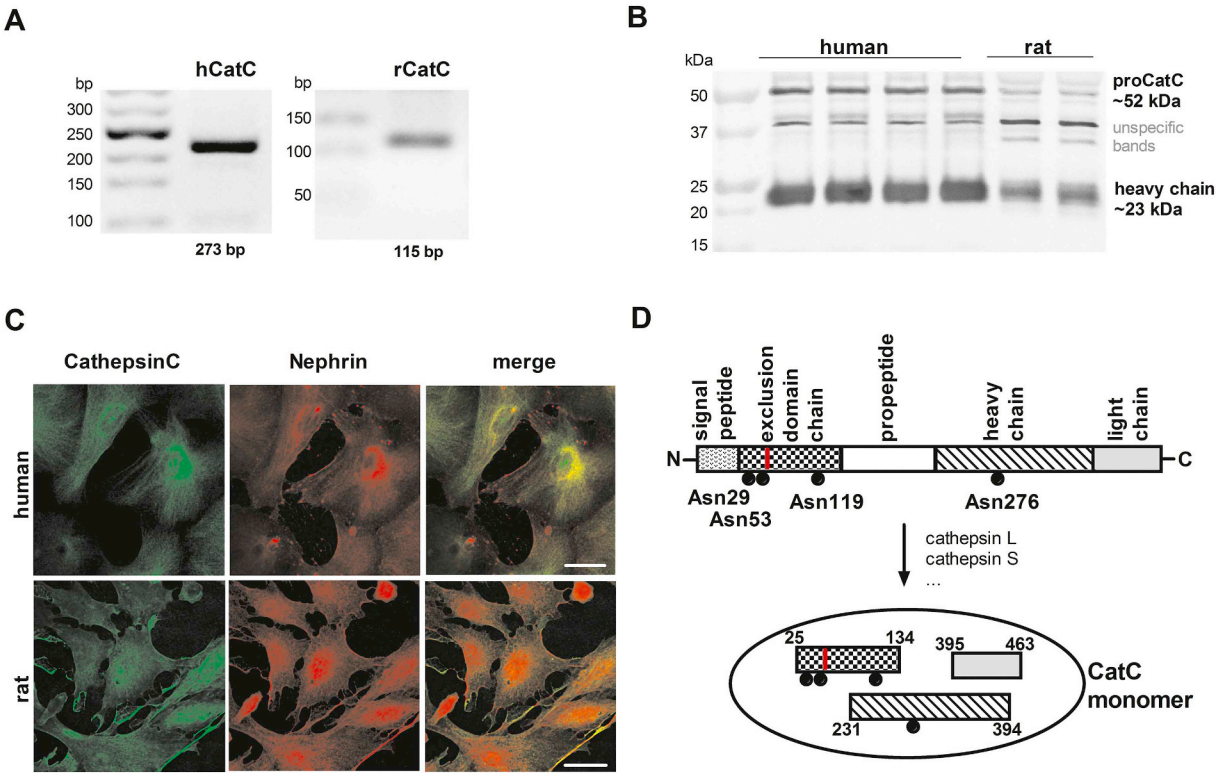

Fig. 2. Cathepsin C expression in immortalized human podocytes and primary rat podocytes. (A) Real-time PCR products visualized on a 2.5% agarose gel and corresponding to the amplified fragments of human and rat CatC mRNA isolated from podocytes. (B) CatC protein expression in human and rat podocytes (in replicates), 25 µg of total protein per lane. (C) Confocal images of CatC and podocyte marker nephrin in human and rat podocytes. Primary antibodies were the same as in the Western blot studies diluted 1:20, fluorescently labeled secondary antibodies were diluted 1:200. Scale bar = 40 µm. (D) Schematic representation of CatC maturation and its subunits.

allowed to stabilize at 37 °C for 1 h. The ECAR values were determined by the Seahorse XFp analyzer (Agilent) before (basic state) and after the injection of 10 mM D-glucose, 1 µM oligomycin, or 50 mM 2-deoxy-D-glucose. The glycolytic flux parameters were obtained from the slopes of the ECAR values in real-time analyses. Baseline and post-exposure rates were measured three times every 3 min (total time ~80 min). The results were normalized to the protein concentrations determined for each cell culture plate well using the Bradford method.

2.13. F-actin network

Alexa Fluor™ 647 Phalloidin (ThermoFisher Scientific) was used to visualize the F-actin network in podocytes cultured on collagen I-coated coverslips. Fluorescence intensity profiles (from basal membrane to nucleus) were generated using NIS-Elements General Analysis 3 software (Nicon). To normalize the fluorescent profiles from different cells, the fluorescence intensity of the X-axis at a distance of 1 µm was expressed as the percentage of the mean value of the fluorescence intensity for the total X-axis and the cell membrane positioned at point 0.

2.14. Statistical analysis

All statistical analyses were performed in GraphPad Prism 8. The Shapiro–Wilk test was used to determine whether parametric or non-parametric tests should be implemented. The results are presented as mean ± SEM. A p-value ≤.05 was considered significant. Statistical tests used in each experiment are shown in Table 3.

3. Results

3.1. Cathepsin C expression and activity are augmented in the urine of diabetic Zucker rats

Zucker rats are a popular model of insulin resistance and metabolic syndrome. The obese (ZO) rats used in experiments (12 weeks old) were slightly hyperglycemic (Supplemental Table 1), but almost all of them exhibited considerable polyuria compared to their lean counterparts (ZL). In proteomic studies, we found that CatC is present in rat urine and its quantity significantly elevated in urine from ZO rats (both proCatC and catalytic forms increased by ~65%; Fig. 1A, B). Furthermore, urine CatC activity was higher in ZO rats than ZL littermates (mean 962 ± 201 A.U. vs. 276 ± 76 A.U., respectively; Fig. 1C). Increased albumin permeability was observed in glomeruli isolated from ZO rats (0.58 ± 0.07 vs. 0.2 ± 0.07 in ZL; Fig. 1D). ZO rats also showed other signs of renal injury, such as increased urine albumin (1.293 ± 0.6 vs. 0.488 ± 0.1; Fig. 1E), nephrin (4.1 ± 0.8 vs. 2.25 ± 0.3; Fig. 8F), and cystatin C (7.16 ± 0.7 vs. 1.9 ± 0.3; Fig. 1G), and decreased levels of urine creatinine (902 ± 51 vs. 1159 ± 82; Fig. 1H).

3.2. Identification of CatC expression in podocytes

We detected CatC expression in both immortalized human podocytes and primary rat podocytes (Fig. 2). Real-time PCR with specific primers designed to span an intron and fluorescent hydrolysis probes resulted in an evident band corresponding to the expected product size (Fig. 2A). In the protein analyses we used mouse monoclonal antibody for better specificity and detected bands corresponding to the zymogen form of CatC (proCatC) and the heavy chain of the catalytically active

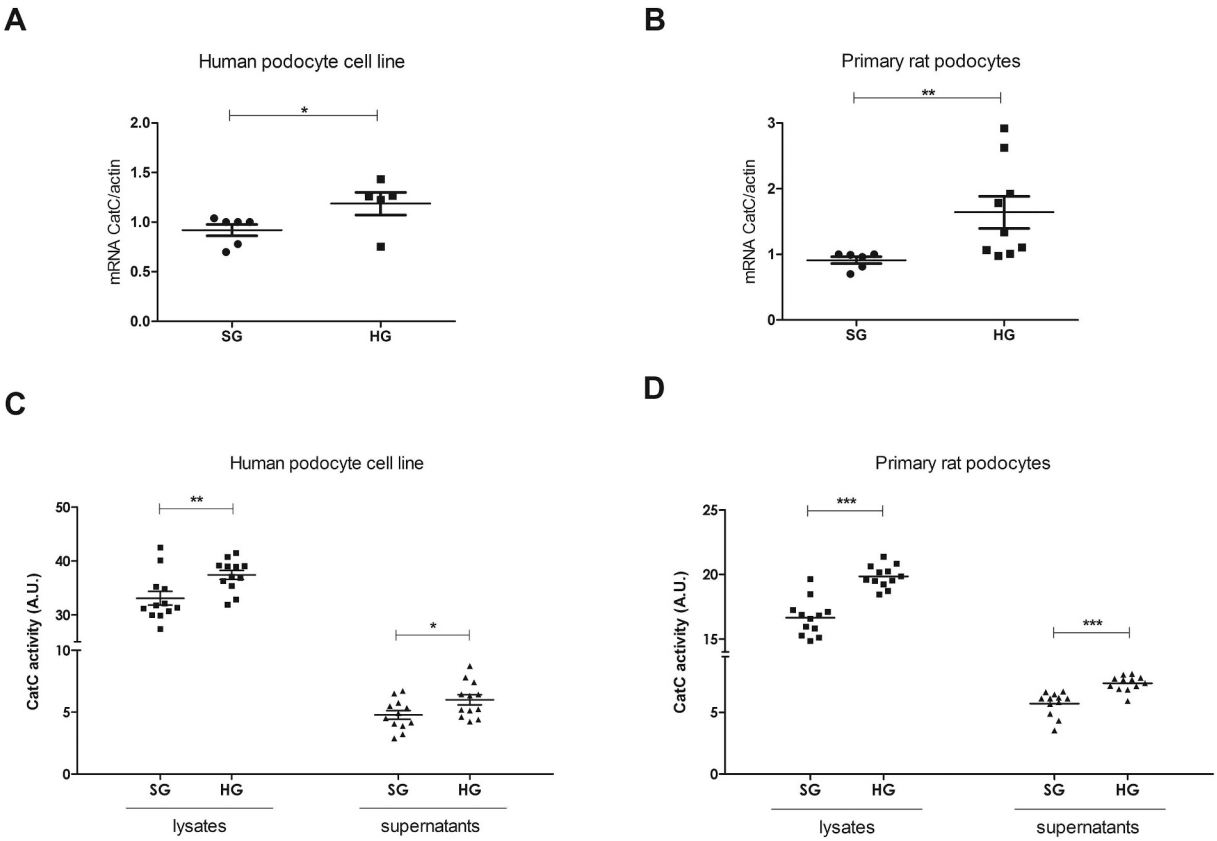

Fig. 3. Cathepsin C is upregulated in the hyperglycemic environment. (A) CatC mRNA levels in immortalized human podocytes cultured in standard glucose medium (SG; 10 mM) and high glucose medium (HG; 30 mM, 5 days) (*p = .055, n = 5–6, unpaired t-test). (B) CatC mRNA levels in primary rat podocytes cultured in SG and HG conditions (**p < .01, n = 6–9, Mann-Whitney test). (C) HG increases intracellular and secreted CatC activity in human podocytes (*p < .05, **p < .01, n = 12, paired t-test). (D) HG stimulates intracellular and secreted CatC activity in primary rat podocytes (***p < .001, n = 12, paired t-test).

CatC heterotrimer (Fig. 2B). The same antibody was used to detect CatC in PFA-fixed podocytes in immunofluorescent studies (Fig. 2C). A schematic of CatC maturation and subunits is presented in Fig. 2D.

3.3. CatC mRNA expression and activity are upregulated in high glucose-cultured podocytes

Cathepsins are emerging as important players in the pathogenesis of diabetic nephropathy; therefore, we analyzed the effects of high glucose concentration (HG; 30 mM, 5 days) on CatC mRNA expression and activity. CatC mRNA levels were increased 29% in human podocytes and 80% in primary rat podocytes under HG conditions (Fig. 3A, B). In addition, CatC activity was elevated 13% and 19% in cell lysates of human and rat podocytes, respectively (Fig. 3C, D). Analyses of CatC activity demonstrated that, in podocytes, CatC is not only expressed intracellularly, but is also secreted outside the cells. We found that CatC activity is significantly higher in cell supernatants obtained from cells cultured in HG conditions, with the values increased 25% and 29% in human and rat cell culture, respectively (Fig. 3C, D).

3.4. HG and PMA stimulate CatC activity and increase albumin permeability in the primary rat podocyte monolayer

PMA is a known activator of the protein kinase C (PKC) family [33], and PKC has been shown to activate cathepsins B, K, and L [34]. Therefore, we examined whether PMA (100 nM, 24 h) (Sigma P1585) stimulates CatC expression and its activity in primary rat podocytes. PMA increased CatC expression by 18% and significantly stimulated CatC activity in lysates (by 48%) and supernatants (by 98%) from primary rat podocytes (Fig. 4A-C). CatC expression and activity were also markedly upregulated in the HG milieu; CatC expression was increased 49%, whereas CatC activity under HG conditions constituted 118% and 130% of the control in lysates and supernatants, respectively (Fig. 4A-C). Interestingly, we did not observe a stronger effect of combined PMA and HG on CatC expression and activity. Furthermore, both PMA and HG significantly augmented albumin permeability in the podocyte monolayer (by 96% after PMA stimulation and by 120% under HG conditions), but there was no additive effect of these factors (Fig. 4D). Cell viability in HG milieu and after PMA treatment was not considerably altered (Supplemental Fig. 4).

3.5. Increased podocyte albumin permeability induced by HG and PMA can be reversed by CatC knockdown

To investigate the potential involvement of CatC in podocyte permeability to albumin, we transfected primary rat podocytes with CatC siRNA and cultured cells in standard medium ± PMA (100 nM, 24 h) or HG medium (30 mM, 5 days). CatC downregulation in all systems was confirmed by Western blot (Fig. 5A). We observed that CatC knockdown partially restored the expression levels of podocyte marker nephrin in cells cultured in HG and after PMA stimulation (Fig. 5B). In addition, CatC depletion reversed the negative effects of both PMA and HG on albumin permeability in podocytes, which was reduced by 19% (SG + PMA siRNA CatC vs. SG + PMA scrambled siRNA, p < .05) and by 32% (HG siRNA CatC vs. HG scrambled siRNA, p < .001; Fig. 5C).

3.6. CatC downregulation ameliorates nephrin, cofilin, and GLUT4 levels in podocytes treated with PMA and HG

Among a variety of different molecular mechanisms of podocyte

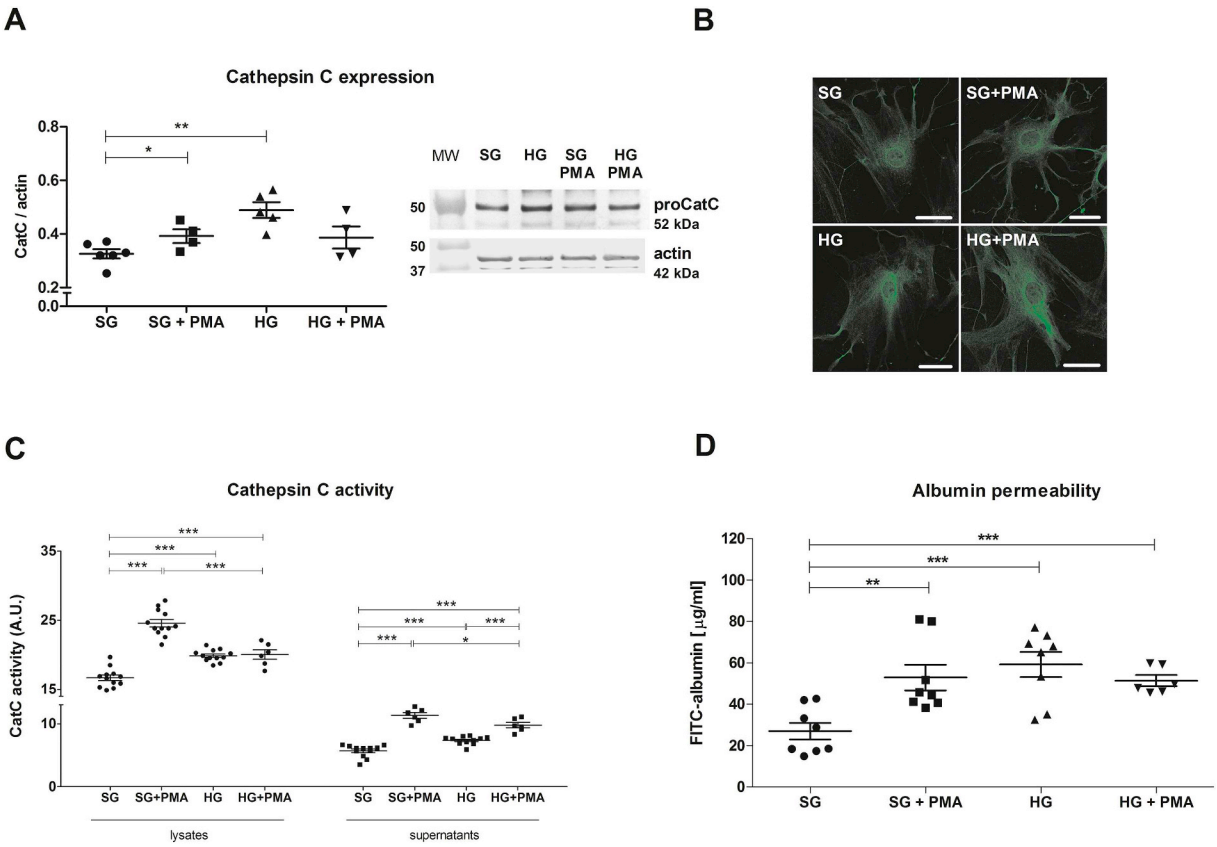

Fig. 4. PMA and HG effects on cathepsin C in primary rat podocytes and their permeability to albumin. (A) Western blot analyses of CatC expression after PMA stimulation (100 nM, 24 h) and in HG (5 days) (*$p < .05$, **$p < .01$, $n = 4–6$, paired *t*-test). (B) Confocal imaging of cathepsin C localization in podocytes cultured in HG or treated with PMA. Scale bar = 50 µm. (C) Cathepsin C activity in podocyte lysates and supernatants after cell exposure to PMA and HG (*$p < .05$, ***$p < .001$, $n = 6–12$, one-way ANOVA). (D) PMA and HG effects on FITC-labeled albumin permeability in the podocyte monolayer (**$p < .01$, ***$p < .001$, n = 6–8, unpaired *t*-test). PMA, phorbol 12-myristate 13-acetate; SG, 11.1 mM D-glucose; HG, 30 mM D-glucose.

injury in HG, rearrangement of the cytoskeleton underlies the increased permeability to albumin in the hyperglycemic milieu. Moreover, abnormal cytoskeletal changes, such as disrupted cofilin-actin interplay, promote the development of insulin resistance [35]. Immunofluorescent staining and confocal imaging showed altered expression of cofilin, an actin-binding protein, and insulin-dependent glucose transporter 4 (GLUT4) after PMA treatment and under HG conditions (Fig. 6A). Despite observing the cofilin signal in the cell bodies and membranes of both control and PMA-treated podocytes, the number of cofilin puncta was markedly reduced in PMA-stimulated cells (Fig. 6A). In contrast, both PMA and HG exposure reduced the GLUT4 signal, especially in the podocyte foot processes and cell membranes (Fig. 6A).

Next, we examined whether downregulation of CatC prevents negative changes exerted by PMA and HG on the expression of GLUT4, cofilin, and the inactive phosphorylated form of cofilin (p-cofilin). In podocytes transfected with CatC siRNA, the expression of GLUT4 and cofilin was ameliorated in PMA and HG-treated podocytes (Fig. 6B-D). The effect of PMA and HG on the levels of p-cofilin was abolished in podocytes with CatC knockdown (Fig. 6E).

3.7. HG and PMA induce cytoskeletal rearrangement in podocytes

To confirm our previous results showing that HG and PMA stimulation trigger cytoskeletal rearrangement in podocytes, we analyzed the F-actin distribution patterns across cells stained with phalloidin. HG and PMA markedly altered intracellular F-actin localization, which was especially concentrated in bundles at the cell membranes (Fig. 7A, B). Moreover, HG and PMA promoted constriction and shrinking of podocyte foot processes (Fig. 7A).

3.8. Glycolytic flux is increased in primary rat podocytes exposed to PMA

Energy metabolism in podocyte foot processes is supported mostly by glycolysis, as mitochondria are physically larger than the lumen of the smallest processes [36]. PMA-induced rearrangement of the cytoskeleton largely alters the morphology of podocytes, especially affecting foot processes. Therefore, we investigated the potential action of PMA and HG on glycolytic flux in primary rat podocytes using real-time recording of ECARs (Fig. 8). Effects of PMA were observed in podocytes cultured in standard glucose (11.1 mM) or high glucose (30 mM; 5 days) before the ECAR analysis. PMA significantly increased glycolysis (56% vs. SG; 74% vs. HG; Fig. 8B), glycolytic capacity (73% vs. SG; 95% vs. HG; Fig. 8C), and glycolytic reserve (76% vs. SG; 106% vs. HG; Fig. 8D) in podocytes, but it did not affect non-glycolytic acidification levels (Fig. 8E).

4. Discussion

The retraction and effacement of podocyte foot processes underlie the disturbance of podocyte function, which plays a central role in the development of proteinuria in diabetic nephropathy. Recently, a number of podocyte proteases that govern the glomerular response to different metabolic states were revealed [4]. Some members of the cathepsin family (cathepsin A, C, D), neprilysin, and neutrophil elastase were also found in the urine exosomes in large-scale proteomic analyses [37,38]. CatC belongs to the cysteine exopeptidases and predominantly localizes in lysosomes/endosomes inside the cells, or is secreted into the extracellular milieu [39]. Some loss-of-function mutations in the CatC gene have been linked to the development of prepubertal periodontosis,

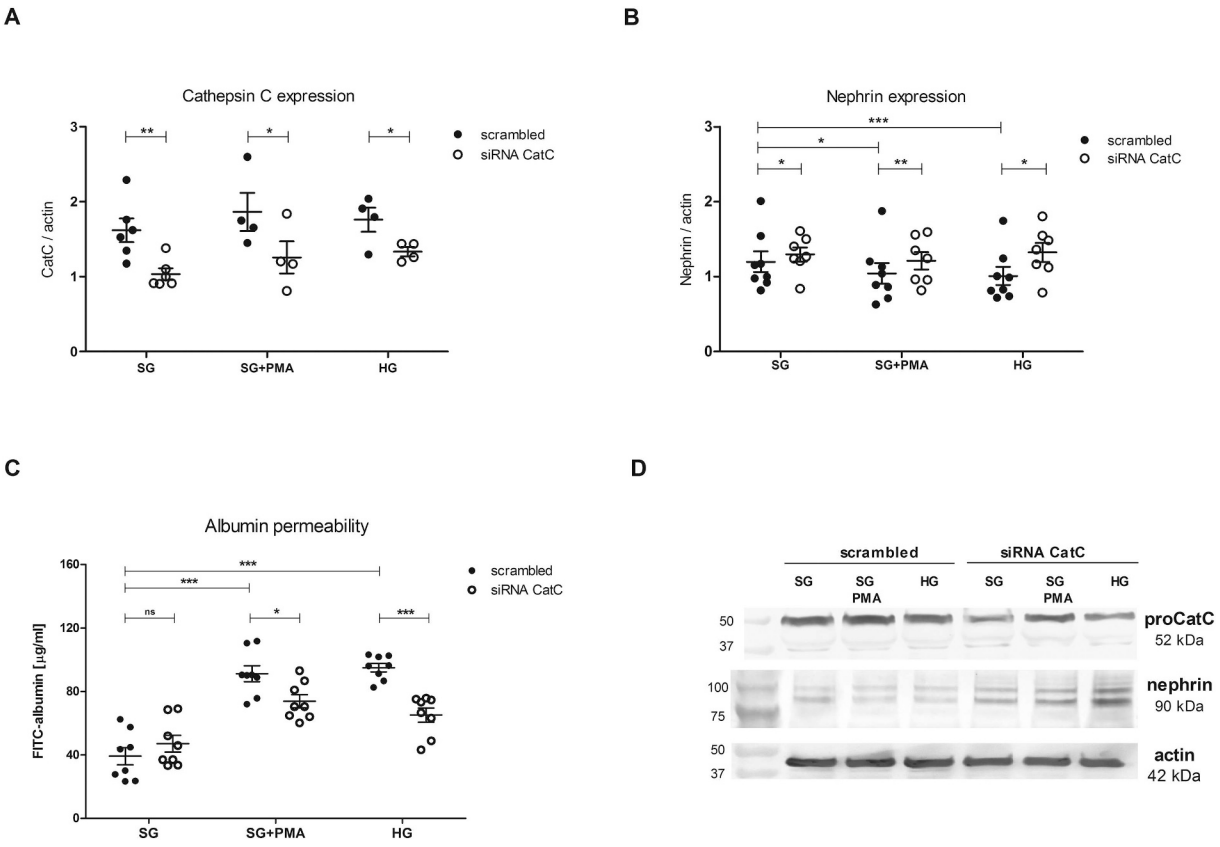

Fig. 5. Cathepsin C downregulation restores nephrin levels and ameliorates albumin permeability in HG and PMA-treated primary rat podocytes. (A) CatC expression after control (scrambled) or CatC siRNA transfection in podocytes stimulated with PMA (100 nM, 24 h) or cultured in HG (5 days) (*$p < .05$, $n = 4$, paired *t*-test, **$p < .01$, $n = 6$, Mann Whitney test). (B) Nephrin expression in podocytes transfected with control or CatC siRNA after HG or PMA exposure (*$p < .05$, **$p < .01$, ***$p < .001$, $n = 7–8$, paired *t*-test). (C) Podocytes transfected with CatC siRNA or control siRNA were subjected to PMA stimulation or were cultured under HG conditions. The FITC-labeled albumin permeability was measured in the podocyte monolayer (*$p < .05$, ***$p < .001$, $n = 8$, Mann Whitney test). (D) Representative blots including actin loading control. PMA, phorbol 12-myristate 13-acetate; SG, 11.1 mM D-glucose; HG, 30 mM D-glucose.

Papillon-Lefèvre syndrome, and aggressive periodontosis [40,41]. Up-regulated CatC activity underlies inflammatory responses in lung diseases, sepsis, and Sendai virus infection [39,42,43]. However, the functional role of CatC in hyperglycemia-associated podocyte injury and its possible involvement in the development of diabetic nephropathy have not been investigated thus far.

In this study, we showed that CatC is expressed in podocytes and secreted into the extracellular space. Interestingly, we observed different intracellular colocalization of CatC and nephrin in human and rat podocytes. In human cells, most mutual spots were in the cytoplasm, whereas in rat cells CatC/nephrin dots overlapped mainly within foot processes and cell membranes, which may be explained by primary podocytes preserving a well-developed web of long and branched foot processes in culture. In contrast, immortalized human podocytes differentiate in vitro and ultimately their morphology is more simple.

As renal damage occurs in diabetes at least in part via alteration of the activity of proteolytic enzymes, we analyzed the levels of CatC expression and activity in podocytes cultured in hyperglycemic medium. The duration of podocyte exposure to HG was set according to our previous reports, in which we showed that, after 5 days in HG-culture, the stimulating effect of insulin on glucose uptake in podocytes is abolished [44,45]. The development of insulin resistance is strongly dependent on the cytoskeletal reorganization and altered function of GLUT1 and GLUT4 [46]. We observed that both PMA (non-specific CatC activator) and HG induce F-actin rearrangements in cultured podocytes, which may lead to morphological changes and disturbances in cell function. We confirmed that elevated CatC expression in podocytes correlates with increased albumin permeability in vitro. Moreover, CatC quantity and activity were significantly higher in urine from ZO rats, along with increased urinary levels of nephrin and albumin. Importantly, CatC depletion markedly ameliorated nephrin and GLUT4 expression in podocytes cultured in the HG milieu, which may improve insulin sensitivity in podocytes [47].

Cysteine peptidases are emerging mediators in many signaling pathways in podocytes, and the effects of their enzymatic activity often involve cytoskeletal rearrangements. Recently, cathepsin L was reported to be overexpressed in several proteinuric kidney diseases, along with increased levels of dynamin, which regulates the actin network and nephrin turnover [48]. Another cysteine peptidase, calpain, is an essential interaction partner for the TRPC6 channel for regulating podocyte motility and adhesion to GBM [3]. Interestingly, we observed significant remodeling of the F-actin network after podocyte stimulation with PMA, a PKC-activating phorbol ester, which also indirectly activates CatC. It seems plausible that the effect of PMA on the podocyte cytoskeleton at least partially depends on cofilin inactivation, which is consistent with several other reports demonstrating altered architecture and the migration of podocytes when cofilin is downregulated [49,50]. In addition, in our recent paper we proposed a molecular mechanism for insulin-dependent translocation of GLUT4 from the cytoplasm to the cell membrane that involves TRPC6/AMPK//Rac1/PAK/cofilin signaling [27]. Here, we showed that the decreased levels of GLUT4 and cofilin in podocytes exposed to HG and PMA can be restored by CatC diminution.

The unique podocyte morphology maintained mainly by the actin cytoskeleton determines the bioenergetic profile of these cells. Evidence supports a dominant role of anaerobic glycolysis, predominantly

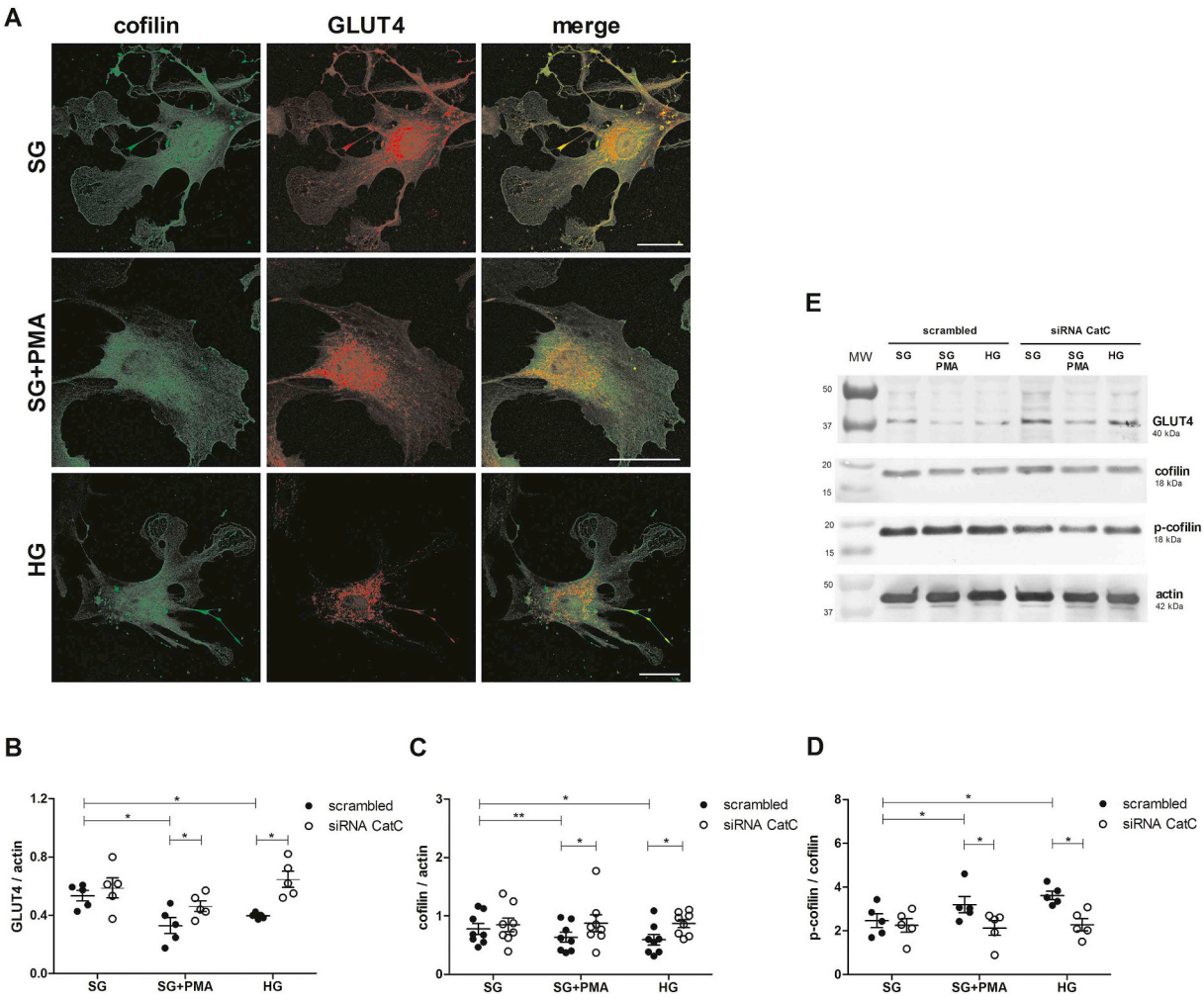

Fig. 6. Cathepsin C downregulation reverses PMA and HG-induced changes in GLUT4 and cofilin expression. (A) Confocal microscopy showing changes in cofilin and GLUT4 signal patterns in primary rat podocytes exposed to PMA (100 nM, 24 h) or cultured in HG (5 days). Scale bar = 40 μm. (B) GLUT4 levels in PMA and HG-treated podocytes were restored in cells transfected with CatC siRNA (*$p < .05$, $n = 5$, paired *t*-test). (C) CatC depletion improves cofilin expression in PMA and HG-treated podocytes (*$p < .05$, **$p < .01$, $n = 8$, paired *t*-test). (D) CatC depletion prevents p-cofilin upregulation in PMA and HG-treated podocytes (*$p < .05$, n = 5, paired *t*-test). (E) Representative blots including actin loading control. PMA, phorbol 12-myristate 13-acetate; SG, 11.1 mM D-glucose; HG, 30 mM D-glucose.

occurring in the foot processes, over oxidative phosphorylation, which is restricted to mitochondria found primarily in the perinuclear region and cell bodies [51]. In other studies and our research, PMA, but not HG, stimulation has been observed to promote the formation of lamellipodia and membrane protrusions in podocytes [52]. Therefore, we investigated whether this morphological alteration is reflected in the glycolysis flux in podocytes. All of the glycolytic parameters were upregulated after PMA treatment, including basic glycolysis, glycolytic capacity, and reserve. The effect of PMA was also retained in podocytes cultured in HG, in which glycolytic flux had a tendency to decline, suggesting a different mechanism of action for both stimuli in glycolysis.

An abnormal podocyte cytoskeletal rearrangement underlies not only increased albumin permeability, but also the development of insulin resistance [53,54]. In our in vivo studies, we employed genetically modified obese Zucker rats, which served as a model of type 2 diabetes, exhibiting improper glucose metabolism and hyperinsulinemia. We demonstrated for the first time that both the activity and expression of CatC is significantly upregulated in the urine of obese Zucker rats. Of course, this does not mean that urinary CatC levels reflect just the podocyte pool of the enzyme, but this finding indicates that CatC may play a role in podocyte function under diabetic conditions, and that it can serve as a marker for renal injury in diabetes. It would be of interest to determine whether higher levels of CatC appear in urine before albuminuria in order to detect renal injury earlier in the course of diabetes and implement appropriate pharmacological treatment to slow the progression of diabetic nephropathy. Additionally, the increased Cystatin C level, together with the decreased urinary creatinine level in Zucker obese rats may reflect not only the podocytes damage, but can be also related to the alteration of other renal structures, e.g. proximal tubules.

In conclusion, the results propose a novel mechanism of podocyte injury in diabetes and provide deeper insight into the role of CatC in podocyte biology. It seems plausible that a better understanding of the pivotal molecular mechanisms contributing to podocyte functioning would provide promising therapeutic targets, which may be pharmacologically or genetically modulated in order to prevent the development of diabetic nephropathy and establish more effective treatments for diabetes.

CRediT authorship contribution statement

Irena Audzeyenka:Conceptualization, Methodology, Investigation, Writing - original draft, Writing - review & editing, Funding acquisition.**Patrycja Rachubik:**Methodology, Investigation, Writing - review & editing.**Dorota Rogacka:**Validation.**Marlena Typiak:**Inv-

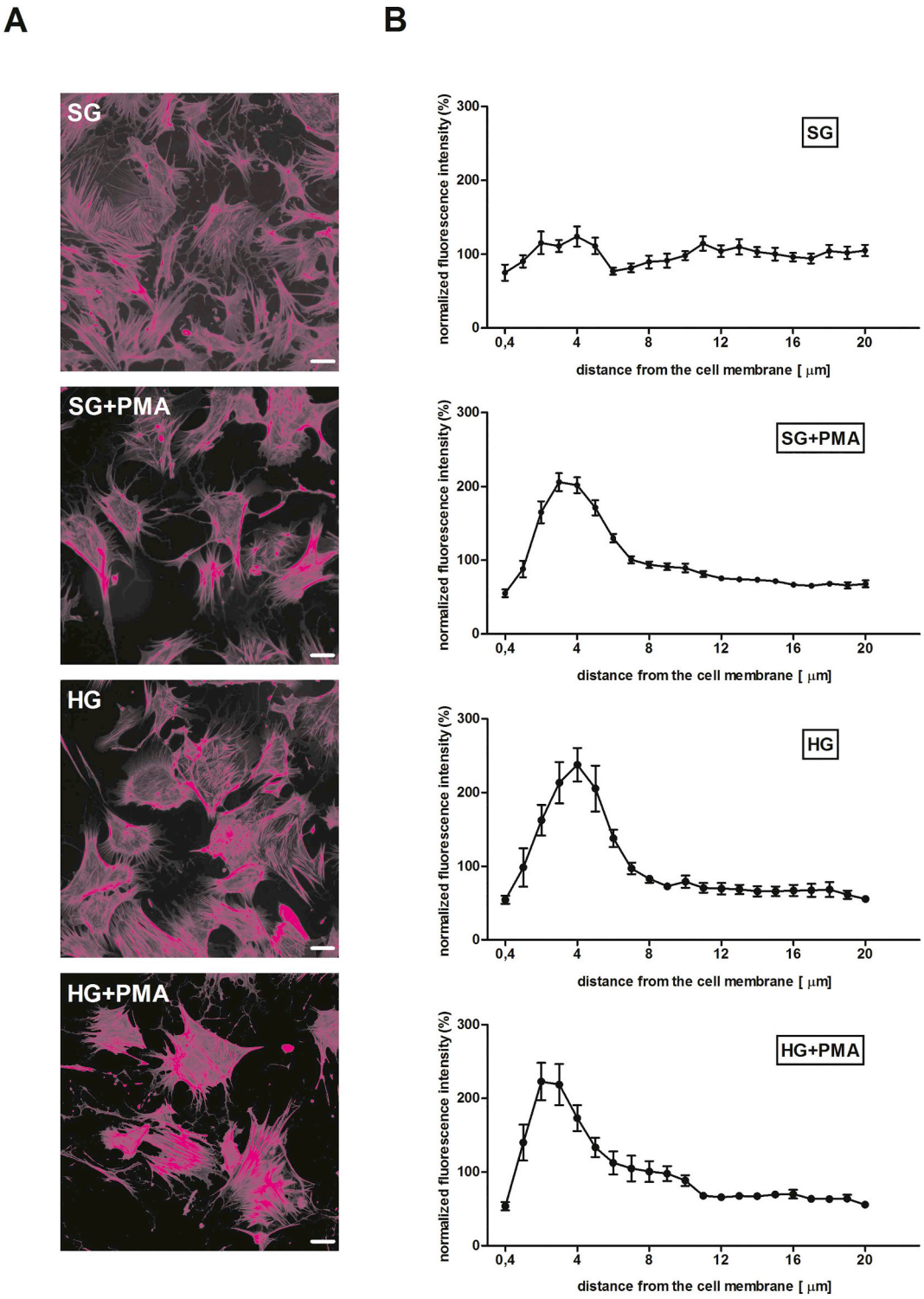

Fig. 7. HG and PMA induce reorganization of the cytoskeleton in primary rat podocytes. (A) Phalloidin-stained podocytes show changes in the F-actin signal patterns after PMA (100 nM, 24 h) and HG (5 days) exposure. Scale bar = 50 μm. (B) The digitized fluorescence images of phalloidin-stained podocytes were used to generate the fluorescence intensity profiles of the F-actin network. All data are presented as mean ± SEM (n = 10–16). PMA, phorbol 12-myristate 13-acetate; SG, 11.1 mM D-glucose; HG, 30 mM D-glucose.

estigation.**Tomasz Kulesza**:Investigation.**Stefan Angielski**:Validation.**Michał Rychłowski**:Investigation.**Magdalena Wysocka**:Conceptualization, Investigation.**Natalia Gruba**:Investigation.**Adam Lesner**:Conceptualization.**Moin A. Saleem**:Validation.**Agnieszka Piwkowska**:Conceptualization, Investigation, Supervision, Funding acquisition.

Declaration of competing interest

The authors declare that they have no known competing financial interests or personal relationships that could have appeared to influence the work reported in this paper.

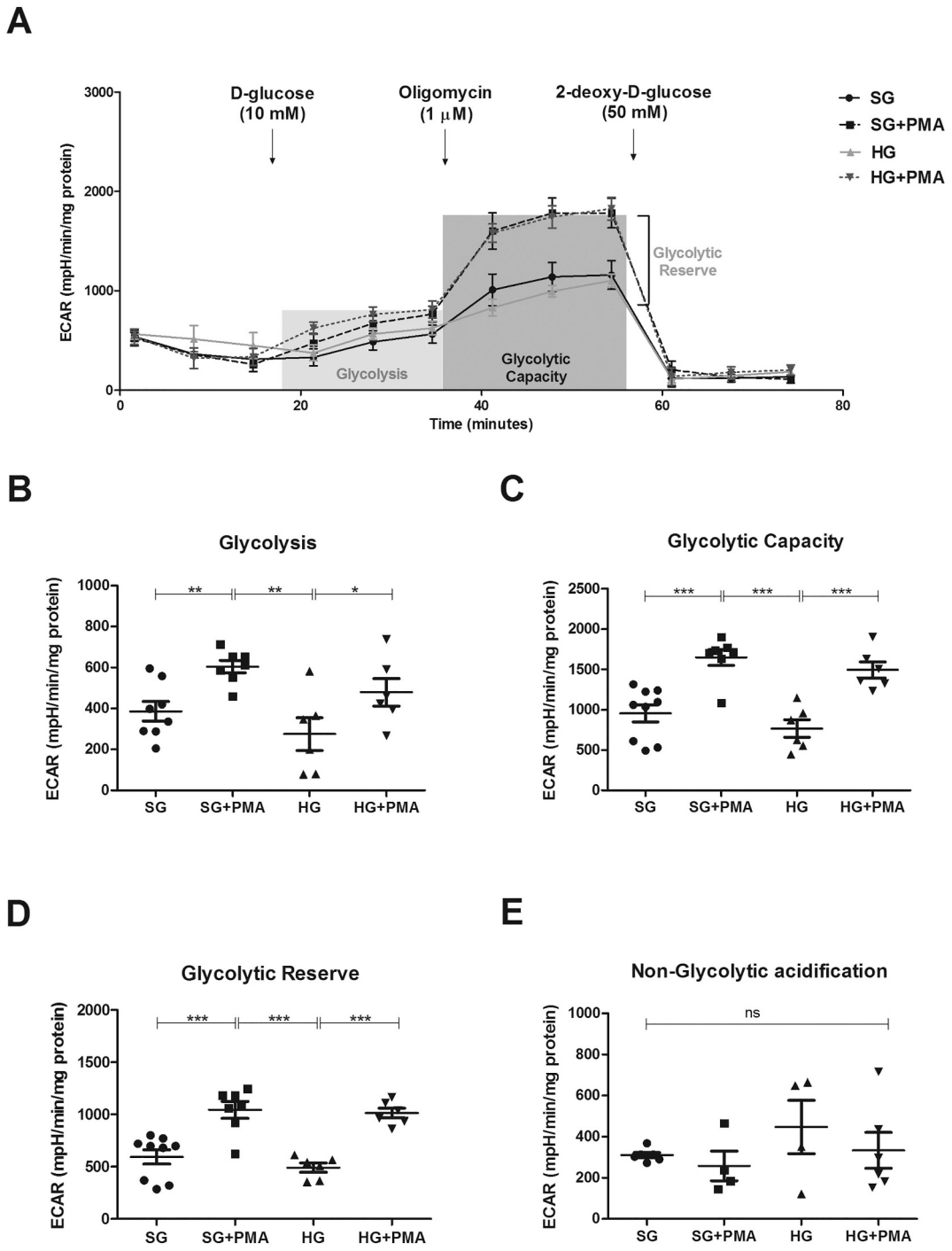

Fig. 8. Glycolytic flux is altered in PMA-treated primary rat podocytes. (A) Extracellular acidification rate of podocytes after PMA stimulation (100 nM, 24 h) and culturing in HG (5 days) after subsequent injection of glucose, oligomycin, and 2-DG. The final concentration of glucose was 10 mM, oligomycin 1 μM, and 2-DG 50 mM. (B) PMA and HG effects on glycolysis in podocytes (**$p < .01$, Mann-Whitney test, *$p < .05$, paired *t*-test, $n = 6–8$). (C) Glycolytic capacity is increased by PMA (***$p < .001$, unpaired *t*-test, n = 6–9). (D) PMA increases the glycolytic reserve ([glycolytic capacity]-[glycolysis]) in podocytes (***$p < .001$, unpaired *t*-test, n = 6–9). (E) Non-glycolytic acidification in podocytes treated with PMA or cultured in HG ($n = 4–6$). PMA, phorbol 12-myristate 13-acetate; SG, 11.1 mM D-glucose; HG, 30 mM D-glucose.

Acknowledgements

This research was supported by grants from the National Science Center (grants 2016/23/D/NZ5/01449 to I. Audzeyenka, and 2014/14/E/NZ4/00358 and 2015/17/B/NZ4/02658 to A. Piwkowska). None of the authors have any competing interests.

Author contributions

I. Audzeyenka, M. Wysocka, A. Lesner, and A. Piwkowska designed the study; I. Audzeyenka, P. Rachubik, M. Typiak, T. Kulesza, M. Rychłowski, M. Wysocka, N. Gruba, and A. Piwkowska carried out the experiments; I. Audzeyenka, P. Rachubik, and A. Piwkowska analyzed the data and prepared the manuscript; D. Rogacka, M. Typiak, S.

Angielski, M. A. Saleem, A. Lesner, and A. Piwkowska revised the manuscript. All authors approved the final version of the manuscript.

Appendix A. Supplementary data

Supplementary data to this article can be found online at https://doi.org/10.1016/j.bbamcr.2020.118723.

References

[1] W.H. Baricos, S.V. Shah, Proteolytic enzymes as mediators of glomerular injury, Kidney Int. 40 (1991) 161–173.

[2] J. Reiser, J. Oh, I. Shirato, K. Asanuma, A. Hug, T.M. Mundel, K. Honey, K. Ishidoh, E. Kominami, J.A. Kreidberg, Y. Tomino, P. Mundel, Podocyte migration during nephrotic syndrome requires a coordinated interplay between cathepsin L and alpha3 integrin, J. Biol. Chem. 279 (2004) 34827–34832.

[3] L.K. Farmer, R. Rollason, D.J. Whitcomb, L. Ni, A. Goodliff, A.C. Lay, L. Birnbaumer, K.J. Heesom, S.Z. Xu, M.A. Saleem, G.I. Welsh, TRPC6 binds to and activates calpain, independent of its channel activity, and regulates podocyte cytoskeleton, cell adhesion, and motility, J. Am. Soc. Nephrol. 30 (10) (2019) 1910–1924.

[4] M.M. Rinschen, A.K. Hoppe, F. Grahammer, M. Kann, L.A. Volker, E.M. Schurek, J. Binz, M. Hohne, F. Demir, M. Malisic, T.B. Huber, C. Kurschat, J.N. Kizhakkedathu, B. Schermer, P.F. Huesgen, T. Benzing, N-Degradomic analysis reveals a proteolytic network processing the podocyte cytoskeleton, J. Am. Soc. Nephrol. 28 (2017) 2867–2878.

[5] A.A. Hasan, B. Hocher, Role of soluble and membrane-bound dipeptidyl peptidase-4 in diabetic nephropathy, J. Mol. Endocrinol. 59 (2017) R1–r10.

[6] M.M. Rinschen, P.F. Huesgen, R.E. Koch, The podocyte protease web: uncovering the gatekeepers of glomerular disease, Am J Physiol Renal Physiol 315 (2018) F1812–f1816.

[7] P. Mundel, J. Reiser, Proteinuria: an enzymatic disease of the podocyte? Kidney Int. 77 (2010) 571–580.

[8] Y. Sharkovska, C. Reichetzeder, M. Alter, O. Tsuprykov, S. Bachmann, T. Secher, T. Klein, B. Hocher, Blood pressure and glucose independent renoprotective effects of dipeptidyl peptidase-4 inhibition in a mouse model of type-2 diabetic nephropathy, J. Hypertens. 32 (2014) 2211–2223.

[9] J.J. Harris, H.J. McCarthy, L. Ni, M. Wherlock, H. Kang, J.F. Wetzels, G.I. Welsh, M.A. Saleem, Active proteases in nephrotic plasma lead to a podocin-dependent phosphorylation of VASP in podocytes via protease activated receptor-1, J. Pathol. 229 (2013) 660–671.

[10] Y. Oe, T. Fushima, E. Sato, A. Sekimoto, K. Kisu, H. Sato, J. Sugawara, S. Ito, N. Takahashi, Protease-activated receptor 2 protects against VEGF inhibitor-induced glomerular endothelial and podocyte injury, Sci. Rep. 9 (2019) 2986.

[11] T. Madhusudhan, H. Wang, B.K. Straub, E. Grone, Q. Zhou, K. Shahzad, S. Muller-Krebs, V. Schwenger, B. Gerlitz, B.W. Grinnell, J.H. Griffin, J. Reiser, H.J. Grone, C.T. Esmon, P.P. Nawroth, B. Isermann, Cytoprotective signaling by activated protein C requires protease-activated receptor-3 in podocytes, Blood 119 (2012) 874–883.

[12] B. Cigic, I. Krizaj, B. Kralj, V. Turk, R.H. Pain, Stoichiometry and heterogeneity of the pro-region chain in tetrameric human cathepsin C, Biochim. Biophys. Acta 1382 (1998) 143–150.

[13] W. Yang, W. Xia, J. Mao, D. Xu, J. Chen, S. Feng, J. Wang, H. Li, C.F. Theisen, J.M. Petersen, M. Thorolfsson, H.B. Rasmussen, F. Junker, E. Boel, J. Su, High level expression, purification and activation of human dipeptidyl peptidase I from mammalian cells, Protein Expr. Purif. 76 (2011) 59–64.

[14] C.T. Pham, R.J. Armstrong, D.B. Zimonjic, N.C. Popescu, D.G. Payan, T.J. Ley, Molecular cloning, chromosomal localization, and expression of murine dipeptidyl peptidase I, J. Biol. Chem. 272 (1997) 10695–10703.

[15] N.V. Rao, G.V. Rao, J.R. Hoidal, Human dipeptidyl-peptidase I. Gene characterization, localization, and expression, J. Biol. Chem. 272 (1997) 10260–10265.

[16] M. Legowska, Y. Hamon, A. Wojtysiak, R. Grzywa, M. Sienczyk, T. Burster, B. Korkmaz, A. Lesner, Development of the first internally-quenched fluorescent substrates of human cathepsin C: the application in the enzyme detection in biological samples, Arch. Biochem. Biophys. 612 (2016) 91–102.

[17] S.W. Dahl, T. Halkier, C. Lauritzen, I. Dolenc, J. Pedersen, V. Turk, B. Turk, Human recombinant pro-dipeptidyl peptidase I (cathepsin C) can be activated by cathepsins L and S but not by autocatalytic processing, Biochemistry 40 (2001) 1671–1678.

[18] Lamort, A. S., Hamon, Y., Czaplewski, C., Gieldon, A., Seren, S., Coquet, L., Lecaille, F., Lesner, A., Lalmanach, G., Gauthier, F., Jenne, D., and Korkmaz, B. (2019) Processing and maturation of cathepsin C zymogen: a biochemical and molecular modeling analysis. *Int J Mol Sci* 20 pii: E4747.

[19] Piwowar, A., Knapik-Kordecka, M., Fus, I., and Warwas, M. (2006) Urinary activities of cathepsin B, N-acetyl-beta-D-glucosaminidase, and albuminuria in patients with type 2 diabetes mellitus. *Med Sci Monit* 12, Cr210-214.

[20] A.L. Sun, J.T. Deng, G.J. Guan, S.H. Chen, Y.T. Liu, J. Cheng, Z.W. Li, X.H. Zhuang, F.D. Sun, H.P. Deng, Dipeptidyl peptidase-IV is a potential molecular biomarker in diabetic kidney disease, Diab. Vasc. Dis. Res. 9 (2012) 301–308.

[21] M. Krochmal, G. Kontostathi, P. Magalhaes, M. Makridakis, J. Klein, H. Husi, J. Leierer, G. Mayer, J.L. Bascands, C. Denis, J. Zoidakis, P. Zurbig, C. Delles, J.P. Schanstra, H. Mischak, A. Vlahou, Urinary peptidomics analysis reveals proteases involved in diabetic nephropathy, Sci. Rep. 7 (2017) 15160.

[22] L.C. Hsing, E.A. Kirk, T.S. McMillen, S.H. Hsiao, M. Caldwell, B. Houston, A.Y. Rudensky, R.C. LeBoeuf, Roles for cathepsins S, L, and B in insulitis and diabetes in the NOD mouse, J. Autoimmun. 34 (2010) 96–104.

[23] M. Packer, Have dipeptidyl peptidase-4 inhibitors ameliorated the vascular complications of type 2 diabetes in large-scale trials? The potential confounding effect of stem-cell chemokines, Cardiovasc. Diabetol. 17 (2018) 9.

[24] S. Gupta, U. Sen, More than just an enzyme: Dipeptidyl peptidase-4 (DPP-4) and its association with diabetic kidney remodelling, Pharmacol. Res. 147 (2019) 104391.

[25] A. Caseiro, R. Ferreira, C. Quintaneiro, A. Pereira, R. Marinheiro, R. Vitorino, F. Amado, Protease profiling of different biofluids in type 1 diabetes mellitus, Clin. Biochem. 45 (2012) 1613–1619.

[26] E. Torban, F. Braun, N. Wanner, T. Takano, P.R. Goodyer, R. Lennon, P. Ronco, A.V. Cybulsky, T.B. Huber, From podocyte biology to novel cures for glomerular disease, Kidney Int. 96 (2019) 850–861.

[27] P. Rachubik, M. Szrejder, D. Rogacka, I. Audzeyenka, M. Rychlowski, S. Angielski, A. Piwkowska, The TRPC6-AMPK pathway is involved in insulin-dependent cytoskeleton reorganization and glucose uptake in cultured rat podocytes, Cell. Physiol. Biochem. 51 (2018) 393–410.

[28] M.A. Saleem, M.J. O'Hare, J. Reiser, R.J. Coward, C.D. Inward, T. Farren, C.Y. Xing, L. Ni, P.W. Mathieson, P. Mundel, A conditionally immortalized human podocyte cell line demonstrating nephrin and podocin expression, J. Am. Soc. Nephrol. 13 (2002) 630–638.

[29] A. Piwkowska, D. Rogacka, M. Jankowski, K. Kocbuch, S. Angielski, Hydrogen peroxide induces dimerization of protein kinase G type Ialpha subunits and increases albumin permeability in cultured rat podocytes, J. Cell. Physiol. 227 (2012) 1004–1016.

[30] V.J. Savin, R. Sharma, H.B. Lovell, D.J. Welling, Measurement of albumin reflection coefficient with isolated rat glomeruli, J. Am. Soc. Nephrol. 3 (1992) 1260–1269.

[31] D. Guay, C. Beaulieu, J.F. Truchon, T. Jagadeeswar Reddy, R. Zamboni, C.I. Bayly, N. Methot, J. Rubin, D. Ethier, M. David Percival, Design and synthesis of dipeptidyl nitriles as potent, selective, and reversible inhibitors of cathepsin C, Bioorg. Med. Chem. Lett. 19 (2009) 5392–5396.

[32] T. Oshima, F.S. Laroux, L.L. Coe, Z. Morise, S. Kawachi, P. Bauer, M.B. Grisham, R.D. Specian, P. Carter, S. Jennings, D.N. Granger, T. Joh, J.S. Alexander, Interferon-gamma and interleukin-10 reciprocally regulate endothelial junction integrity and barrier function, Microvasc. Res. 61 (2001) 130–143.

[33] L. Ambrus, A. Olah, T. Olah, G. Balla, M.A. Saleem, P. Orosz, J. Zsuga, K. Biro, L. Csernoch, T. Biro, T. Szabo, Inhibition of TRPC6 by protein kinase C isoforms in cultured human podocytes, J. Cell. Mol. Med. 19 (2015) 2771–2779.

[34] A. Ruettger, S. Schueler, J.A. Mollenhauer, B. Wiederanders, Cathepsins B, K, and L are regulated by a defined collagen type II peptide via activation of classical protein kinase C and p38 MAP kinase in articular chondrocytes, J. Biol. Chem. 283 (2008) 1043–1051.

[35] T.T. Chiu, N. Patel, A.E. Shaw, J.R. Bamburg, A. Klip, Arp2/3- and cofilin-coordinated actin dynamics is required for insulin-mediated GLUT4 translocation to the surface of muscle cells, Mol. Biol. Cell 21 (2010) 3529–3539.

[36] S. Ozawa, S. Ueda, H. Imamura, K. Mori, K. Asanuma, M. Yanagita, T. Nakagawa, Glycolysis, but not mitochondria, responsible for intracellular ATP distribution in cortical area of podocytes, Sci. Rep. 5 (2015) 18575.

[37] P.A. Gonzales, T. Pisitkun, J.D. Hoffert, D. Tchapyjnikov, R.A. Star, R. Kleta, N.S. Wang, M.A. Knepper, Large-scale proteomics and phosphoproteomics of urinary exosomes, J. Am. Soc. Nephrol. 20 (2009) 363–379.

[38] M.C. Hogan, K.L. Johnson, R.M. Zenka, M.C. Charlesworth, B.J. Madden, D.W. Mahoney, A.L. Oberg, B.Q. Huang, A.A. Leontovich, L.L. Nesbitt, J.L. Bakeberg, D.J. McCormick, H.R. Bergen, C.J. Ward, Subfractionation, characterization, and in-depth proteomic analysis of glomerular membrane vesicles in human urine, Kidney Int. 85 (2014) 1225–1237.

[39] Y. Hamon, M. Legowska, V. Herve, S. Dallet-Choisy, S. Marchand-Adam, L. Vanderlynden, M. Demonte, R. Williams, C.J. Scott, M. Si-Tahar, N. Heuze-Vourc'h, G. Lalmanach, D.E. Jenne, A. Lesner, F. Gauthier, B. Korkmaz, Neutrophilic cathepsin C is maturated by a multistep proteolytic process and secreted by activated cells during inflammatory lung diseases, J. Biol. Chem. 291 (2016) 8486–8499.

[40] C. Toomes, J. James, A.J. Wood, C.L. Wu, D. McCormick, N. Lench, C. Hewitt, L. Moynihan, E. Roberts, C.G. Woods, A. Markham, M. Wong, R. Widmer, K.A. Ghaffar, M. Pemberton, I.R. Hussein, S.A. Temtamy, R. Davies, A.P. Read, P. Sloan, M.J. Dixon, N.S. Thakker, Loss-of-function mutations in the cathepsin C gene result in periodontal disease and palmoplantar keratosis, Nat. Genet. 23 (1999) 421–424.

[41] C. Hewitt, D. McCormick, G. Linden, D. Turk, I. Stern, I. Wallace, L. Southern, L. Zhang, R. Howard, P. Bullon, M. Wong, R. Widmer, K.A. Gaffar, L. Awawdeh, J. Briggs, R. Yaghmai, E.W. Jabs, P. Hoeger, O. Bleck, S.G. Rudiger, G. Petersilka, M. Battino, P. Brett, F. Hattab, M. Al-Hamed, P. Sloan, C. Toomes, M. Dixon, J. James, A.P. Read, N. Thakker, The role of cathepsin C in Papillon-Lefevre syndrome, prepubertal periodontitis, and aggressive periodontitis, Hum. Mutat. 23 (2004) 222–228.

[42] A.M. Akk, P.M. Simmons, H.W. Chan, E. Agapov, M.J. Holtzman, M.H. Grayson, C.T. Pham, Dipeptidyl peptidase I-dependent neutrophil recruitment modulates the inflammatory response to Sendai virus infection, J. Immunol. 180 (2008) 3535–3542.

[43] J. Mallen-St Clair, C.T. Pham, S.A. Villalta, G.H. Caughey, P.J. Wolters, Mast cell dipeptidyl peptidase I mediates survival from sepsis, J. Clin. Invest. 113 (2004) 628–634.

[44] D. Rogacka, A. Piwkowska, I. Audzeyenka, S. Angielski, M. Jankowski, Involvement of the AMPK-PTEN pathway in insulin resistance induced by high glucose in cultured rat podocytes, Int. J. Biochem. Cell Biol. 51 (2014) 120–130.

[45] D. Rogacka, A. Piwkowska, I. Audzeyenka, S. Angielski, M. Jankowski, SIRT1-

AMPK crosstalk is involved in high glucose-dependent impairment of insulin responsiveness in primary rat podocytes, Exp. Cell Res. 349 (2016) 328–338.
[46] R.J. Coward, G.I. Welsh, J. Yang, C. Tasman, R. Lennon, A. Koziell, S. Satchell, G.D. Holman, D. Kerjaschki, J.M. Tavare, P.W. Mathieson, M.A. Saleem, The human glomerular podocyte is a novel target for insulin action, Diabetes 54 (2005) 3095–3102.
[47] R.J. Coward, G.I. Welsh, A. Koziell, S. Hussain, R. Lennon, L. Ni, J.M. Tavare, P.W. Mathieson, M.A. Saleem, Nephrin is critical for the action of insulin on human glomerular podocytes, Diabetes 56 (2007) 1127–1135.
[48] R. Khalil, K. Koop, R. Kreutz, H.P. Spaink, P.C. Hogendoorn, J.A. Bruijn, H.J. Baelde, Increased dynamin expression precedes proteinuria in glomerular disease, J. Pathol. 247 (2019) 177–185.
[49] P. Garg, R. Verma, L. Cook, A. Soofi, M. Venkatareddy, B. George, K. Mizuno, C. Gurniak, W. Witke, L.B. Holzman, Actin-depolymerizing factor cofilin-1 is necessary in maintaining mature podocyte architecture, J. Biol. Chem. 285 (2010) 22676–22688.
[50] S. Ashworth, B. Teng, J. Kaufeld, E. Miller, I. Tossidou, C. Englert, F. Bollig, L. Staggs, I.S. Roberts, J.K. Park, H. Haller, M. Schiffer, Cofilin-1 inactivation leads to proteinuria–studies in zebrafish, mice and humans, PLoS One 5 (2010) e12626.
[51] P.T. Brinkkoetter, T. Bork, S. Salou, W. Liang, A. Mizi, C. Ozel, S. Koehler, H.H. Hagmann, C. Ising, A. Kuczkowski, S. Schnyder, A. Abed, B. Schermer, T. Benzing, O. Kretz, V.G. Puelles, S. Lagies, M. Schlimpert, B. Kammerer, C. Handschin, C. Schell, T.B. Huber, Anaerobic glycolysis maintains the glomerular filtration barrier independent of mitochondrial metabolism and dynamics, Cell Rep. 27 (2019) 1551–1566.
[52] T. Bondeva, S. Wojciech, G. Wolf, Advanced glycation end products inhibit adhesion ability of differentiated podocytes in a neuropilin-1-dependent manner, Am J Physiol Renal Physiol 301 (2011) F852–F870.
[53] A.A. Wasik, S. Koskelainen, M.E. Hyvonen, L. Musante, E. Lehtonen, K. Koskenniemi, J. Tienari, A. Vaheri, D. Kerjaschki, C. Szalay, C. Revesz, P. Varmanen, T.A. Nyman, P. Hamar, H. Holthofer, S. Lehtonen, Ezrin is downregulated in diabetic kidney glomeruli and regulates actin reorganization and glucose uptake via GLUT1 in cultured podocytes, Am. J. Pathol. 184 (2014) 1727–1739.
[54] C. Martinez-Garcia, A. Izquierdo-Lahuerta, Y. Vivas, I. Velasco, T.K. Yeo, S. Chen, G. Medina-Gomez, Renal lipotoxicity-associated inflammation and insulin resistance affects actin cytoskeleton organization in podocytes, PLoS One 10 (2015) e0142291.